An exciton on coupled concentric double nanorings in a magnetic field

2008 J. Phys.: Condens. Matter 20 365222

(http://iopscience.iop.org/0953-8984/20/36/365222)

J. Phys.: Condens. Matter **20** (2008) 365222 (8pp) doi:10.1088/0953-8984/20/36/365222

An exciton on coupled concentric double nanorings in a magnetic field

Weiwei Song, Guojun Jin and Yu-qiang Ma

National Laboratory of Solid State Microstructures and Department of Physics, Nanjing University, Nanjing 210093, People's Republic of China

E-mail: gjin@nju.edu.cn

Received 21 May 2008, in final form 6 August 2008
Published 20 August 2008
Online at stacks.iop.org/JPhysCM/20/365222

Abstract

We study the influence of coupling between two concentric nanorings, embedded in two different layers separated by an insulating barrier, on the exciton's energy levels by the attractive Fermionic Hubbard model. The hopping coefficients between different rings are derived and the carriers' cyclotron movement caused by the magnetic field are taken into account. We find the amplitude of the Aharonov–Bohm oscillation is suppressed by the emergence of the Coulomb interaction. The coupling leads to a decrease of the energy of the excited states and this decrease varies significantly for different types of configuration for the electron and the hole. The study of the energy dependence on the radii of the two rings shows that the lowest energy level is determined by the small ring and the deviations of the exciton's energy from that of the single ring decreases with increasing magnetic field. The results also show that the energy of the AB oscillation can be modulated by changing the thickness of the spacer.

1. Introduction

In recent years, following the advancement in nanoscopic fabrication techniques [1–4], the properties of the ring-like semiconductor nanostructures, also called nanorings or quantum rings, have attracted much attention. In these nanostructures, the electronic and optical properties are strongly modified from those of solids by the quantum confinement, which provides us more opportunities to control, develop and apply new artificial materials. As one of the most important properties, when a nanoring is penetrated by a magnetic field, it shows an Aharonov–Bohm (AB) oscillation in the binding energy, which has been studied experimentally [5, 6] and theoretically by a single electron model [7, 8] and the confined exciton model [9–12]. The effects of the lateral applied steady electric field [13] and alternating electric field [14] have also been studied.

It has been shown experimentally that the strong coupling between nanorings can greatly influence the photoluminescence (PL) spectra of the system. Granados *et al* [3] studied the PL spectra of stacked layers of self-assembled InGaAs nanorings with various GaAs spacers between those layers. The samples show strong inhomogeneous broadened and redshifted spectra when the thickness of the GaAs spacer is smaller than 4.5 nm. The authors attribute these phenomena to the broad size distribution and the coupling between layers. Mano *et al* [4] reported the self-assembled formation of concentric quantum double rings. Ouerghui *et al* [15] studied the effect of coupling on the exciton radiative lifetime of a similar configuration and pointed out that the PL spectra measured can be attributed to a bimodal size distribution of the nanoring ensemble.

In the present paper, we generalize the theoretical work conducted by Palmero *et al* [16] to the coupling rings and mainly concentrate on the coupling effect on an exciton's energy levels for two concentric rings embedded in two parallel layers. The hopping coefficients between rings are derived in a new form. The discussions are focused on the AB oscillation of excitonic levels and the influence of geometrical parameters on the energy levels. The rest of the paper is organized as follows: section 2 concerns the theoretical model and analysis. Presented in section 3 are the numerical results for the dependence of excitonic levels on magnetic field and geometrical parameters of the system. Finally, a summary is given in section 4.

2. Theoretical model and analysis

The system we consider here is made up of two coupling semiconductor rings that are embedded in two parallel layers

and are penetrated by a uniform magnetic field. The material between these two layers is GaAs. Without taking into account the spin–orbit coupling, the spin-dependent part of the Hamiltonian is in a linear form with the magnetic field [17], so it just provides a linear addition to the total energy of the system. For the convenience of calculation, we restrict our model to coupling a one dimensional ring system with a spinless electron and a spinless hole.

Each ring, considered in our model, consists of two series of sites, one for electrons, the other for holes, and each series consists of M sites which are equally spaced in each ring, as sketched in figure 1. The thickness of the spacer is taken as d. We assume that the Coulomb potential is short range and consider the interaction only when the electron and the hole are in the same layer. The system can be described by the attractive Fermionic Hubbard model [16, 18]. We also assume that the particles can only hop between the nearest neighboring sites. So the Hamiltonian of the system reads

$$\mathcal{H} = \mathcal{H}_{\rm int} + \mathcal{H}_{\perp} + \mathcal{H}_{\parallel}, \tag{1}$$

where $\mathcal{H}_{\rm int}$, $\mathcal{H}_{\perp}$ and $\mathcal{H}_{\parallel}$ represent the interaction between the electron and the hole, the hopping between different rings, and the hopping contribution between nearest neighboring sites on a same ring, respectively. They can be written as

$$\mathcal{H}_{\rm int} = -\sum_{i=1}^{2}\sum_{j,l=1}^{M} \gamma_{(d_{j,l})} a^{\dagger}_{i,j} a_{i,j} b^{\dagger}_{i,l} b_{i,l}, \tag{2}$$

$$\mathcal{H}_{\perp} = -\sum_{i=1}^{2}\sum_{j=1}^{M} (t^{\perp}_{i,\rm e} {\rm e}^{2{\rm i}\pi\varphi_{\rm e}} a^{\dagger}_{i,j} a_{i+1,j} + t^{\perp}_{i,\rm h} {\rm e}^{2{\rm i}\pi\varphi_{\rm h}} b^{\dagger}_{i,j} b_{i+1,j} + {\rm h.c.}), \tag{3}$$

$$\mathcal{H}_{\parallel} = -\sum_{i=1}^{2}\sum_{j=1}^{M} [t^{\parallel}_{i} {\rm e}^{2{\rm i}\pi\varphi_i/M} (a^{\dagger}_{i,j} a_{i,j+1} + \mu b^{\dagger}_{i,j+1} b_{i,j}) + {\rm h.c.}], \tag{4}$$

where $a^{\dagger}_{i,j}$ ($a_{i,j}$) creates (annihilates) an electron at site j on the ith ring. Similarly, $b^{\dagger}_{i,l}$ ($b_{i,l}$) is the creation (annihilation) operator for a hole at the corresponding sites. The parameter $\gamma_{(d_{j,l})}$ represents the intensity of the interaction between the electron on site j and the hole on site l, where $d_{j,l}$ represents the distance of these two particles. The symbol $t^{\perp}_{i,\rm e(h)}$ represents the hopping coefficient of the electron (hole) between neighboring sites on different rings. $2\pi\varphi_{\rm e}$ ($2\pi\varphi_{\rm h}$) represents the change of the electron's (hole's) Aharonov–Bohm phase, which is introduced by the deflection from its original position (the position with no external magnetic field), when hopping between different rings. The parameter $t^{\parallel}_{i}$ means the electron's hopping coefficient between neighboring sites along the ith ring. The symbol φ_i represents the magnetic flux through the ith ring, in the unit of the flux quantum, hc/e. μ represents the ratio of the effective masses of the electron and the hole in the InGaAs material which makes up the nanorings.

From the original definition of the hopping matrix element [19],

$$t_{ij} = \frac{\hbar^2}{2m^*} \int \psi^*_i(\boldsymbol{x}) \bigtriangledown^2 \psi_j(\boldsymbol{x})\, {\rm d}\boldsymbol{x}, \tag{5}$$

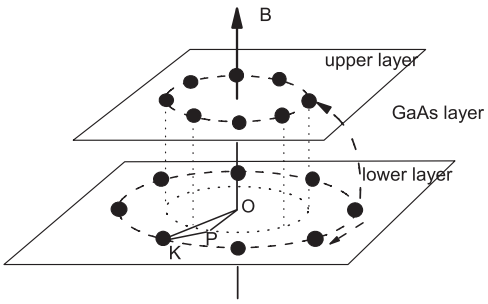

Figure 1. Sketch of two concentric nanorings embedded in two layers separated by a spacer. Each ring consists of M sites in which electrons (holes) can hop between the nearest neighboring sites. The system is penetrated by a uniform magnetic field.

where ψ_i is the wavefunction at site i, we can get the hopping coefficient in the same ring as [11, 16]

$$t^{\parallel}_{i} = \frac{\hbar^2}{2m^*} \frac{\epsilon_0}{4r_i^2 \sin^2(\pi/M)}, \tag{6}$$

where r_i ($i = 1, 2$) represents the nanoring radius (r_1 for the small ring and r_2 for the large ring), and ϵ_0 is related to the properties of materials.

For the hopping coefficient between different rings, using the variable separation technique, $t^{\perp}_{i,\rm e(h)}$ can be divided into two parts $t^{\perp z}_{i,\rm e(h)}$ and $t^{\perp(\rho\theta)}_{i,\rm e(h)}$ according to the symmetry of the system. The former is proportional to the hopping coefficient between the two layers where the rings are embedded. Using the finite square well potential approximation along the z direction, we find

$$t^{\perp z}_{i,\rm e(h)} = \frac{\hbar^2}{2m^*} \beta^2 {\rm e}^{-\beta d} \frac{\chi\epsilon_1}{\frac{1}{\beta d} + \frac{1}{1+\cos(k_z h)}\left[\frac{h}{d} + \frac{\sin(k_z h)}{k_z d}\right]}, \tag{7}$$

where k_z is the wavevector along the z direction in the ring, h is the height of the ring along the z direction, d is the thickness of the GaAs spacer and β is the attenuation constant in the spacer, which is determined by the energy of the particle in the finite square well along the z direction and height of the barrier, V_0. The parameter χ is the overlap integral of the wavefunction in the (ρ, θ) plane and ϵ_1 is the parameter that is related to the properties of materials. Carefully analyzing $t^{\perp z}_{i,\rm e(h)}$, we can find that it is a product of the particle's energy and the overlap integral of the wavefunctions in different layers.

For the latter part of the hopping coefficient between different rings, $t^{\perp(\rho\theta)}_{i,\rm e(h)}$, because particles are confined in two regions along the ρ direction, it is reasonable to assume that it has a similar form as the former part described above. According to the data used in [3] and [17], the typical width of rings along the ρ direction is much larger than the height, h, so the ground state energy of particles in the ρ direction can be approximately taken as $-V_0$ taking the GaAs barrier as the zero point of energy. We can get $t^{\perp}_{i,\rm e(h)}$ in the form

$$t^{\perp}_{i,\rm e(h)} = \frac{\hbar^2}{2m^*} \left(\beta^2 + \beta'^2\right) {\rm e}^{-(\beta d + \beta' \Delta l)} \beta' \Delta l \times \frac{\epsilon_1}{\frac{1}{\beta d} + \frac{1}{1+\cos(k_z h)}\left[\frac{h}{d} + \frac{\sin(k_z h)}{k_z d}\right]}. \tag{8}$$

Here we take the median value of the inner and outer radii of one ring as the radius to calculate the coupling. It is also convenient to use this method to calculate the coupling between rings with finite width by dividing one ring into several concentric rings, as in [16], each of which can be viewed as a quasi-one-dimensional ring. β' is the attenuation constant of the wavefunction in the (ρ, θ) plane, taken as $\sqrt{2m^*V_0}/\hbar$. Δl, the length of KP in figure 1, is the projected distance of the nearest neighboring sites on different rings and can be calculated.

For the parameter φ_e (φ_h), it is necessary to calculate the electron's (hole's) deflection from the original position, which means the position it is supposed to reach when hopping without external magnetic field. Here we use the semiclassical method to calculate this deflection. Using the result in [20, 21], we can get the average particle time for one particle to get through the single rectangular barrier under zero bias as

$$\tau = \frac{\hbar}{8(V_0 - E_0)\sqrt{E_0(V_0 - E_0)}} \times [V_0 \sinh(2\beta d) + 2\beta d(V_0 - 2E_0)] \tag{9}$$

where E_0 is the particle's energy. It is noted that τ represents the transmission time of the particle to cross through the GaAs layer [21].

It is reasonable to divide the tunneling process into two parts by the variable separation method, one along the z direction, the other in the (ρ, θ) plane. We take the GaAs layer as homogeneous, then we can get the deflection of the particle from τ. In the form of radians, it reads:

$$\Delta\vartheta = \arccos\frac{r_2 - r\sin\theta}{r_1}, \tag{10}$$

where $\theta = qB\tau/m^*$ represents the angle that the particle moves in its cyclotron movement from the site on the large ring, and r is the cyclotron radius of the particle and reads:

$$r = r_2\frac{\sin\theta - \sqrt{\sin^2\theta - 2(1-\cos\theta)(1-(r_1/r_2)^2)}}{1-\cos\theta}. \tag{11}$$

Here we have to take into account the restriction emerging from the system's configuration. The first one is that the cyclone radius r should be larger than the difference of the radii of the two rings, which ensures that the particle can jump from one ring to the other one. The second one is that $r_1/r_2 > \sin(\theta/2)$ which ensures the solvability of equation (11). These restrictions can also influence the hopping coefficients: when $r < \Delta r_{12}$ or $r_1/r_2 < \sin(\theta/2)$, the parameter $t^{\perp}_{i,e(h)}$ should be taken as 0 because the particles can not reach the smaller ring when hopping from the bigger ring.

To ensure the hermitian symmetry of the Hamiltonian, we make the assumption that the hopping is reversible, which means we just take into account the flux in the area ΔKPO in figure 1 when calculating the change of the AB phase as the particles hop between different rings. It must be made clear that the neighboring sites on different rings here mean the corresponding neighboring sites at zero magnetic field. When a magnetic field is added perpendicular to the rings, this neighboring relationship will not be affected.

For the convenience of calculation, we take the sites on the large ring as stationary and the sites on the small ring have a constant deflection from their original positions when an external magnetic field is applied. The two series of sites (for electrons and for holes) on the large ring is chosen to coincide with each other, as in [16, 11]. For the sites on the small ring, at zero field, we choose the jth site on the plane that is determined by the jth site on the large ring and the centers of two rings. However, if an external magnetic field is applied to the system, when hopping between different rings, the electron and the hole will deflect in opposite directions due to their different signs of charge, so the sites on the small ring, which carry two states (one for electrons and the other for holes) at zero field, will be split into two sites that are separated by a constant distance, which means the small ring will contain two separated series of sites: one for electrons and one for holes.

We consider the interaction between particles only when they are in the same layer and assume the Coulomb potential to be short range [16], by taking the cut-off radius to be $r_1\sin(\pi/M)$. On the other hand, from the system's symmetry, the Coulomb potential should be invariable with the change of its position [13]. Hence the Coulomb potential is taken with the form of a square well:

$$V_{(d_{j,l})} = \begin{cases} -\gamma_0, & \text{for } d_{j,l} \leqslant r_1\sin(\pi/M); \\ 0, & \text{for } d_{j,l} > r_1\sin(\pi/M). \end{cases} \tag{12}$$

Here γ_0 is the intensity of the interaction when the electron and the hole are on the same site [16], $d_{j,l}$ represents the distance of the site with an electron from the nearest site with a hole. The unit of the parameter γ_0 is chosen to be the electron hopping energy in the smaller ring, $\hbar^2\epsilon_0/4m^*r_1^2\sin^2(\pi/M)$, as in [16]. For the parameters $\boldsymbol{\epsilon}_1$ in equation (8), we generally take it as $\boldsymbol{\epsilon}_1 = 1$.

In [22], Scott provides us the number-state method to get the eigenvalues of the Schrödinger equation. This method has been widely applied to the investigation of the Hubbard model [18]. Using this method, excitons in a finite-width nanoring are studied by Palmero [16]. In this paper, we will use this number-state method to study a system with two different sized nanorings embedded in two different layers. The number-state base vector is chosen in the form:

$$\left|\begin{matrix} n^h_{11}, n^h_{12}, \ldots, n^h_{1M}; n^h_{21}, n^h_{22}, \ldots, n^h_{2M} \\ n^e_{11}, n^e_{12}, \ldots, n^e_{1M}; n^e_{21}, n^e_{22}, \ldots, n^e_{2M} \end{matrix}\right\rangle. \tag{13}$$

Here, n^e_{ij} (n^h_{ij}) represents the number of the electron (hole) in the jth site on the ith ring. We assume that the number of electrons and that of holes are conservative and both of them are equal to one. Because of the rotation symmetry of the system, a general eigenfunction can be written as

$$|\psi_{2,\tau_0}\rangle = \sum_{i=1}^{4}\sum_{m=1}^{M} c^i_m|\psi^i_m\rangle \tag{14}$$

where

$$|\psi^1_m\rangle = \frac{1}{\sqrt{M}}\sum_{j=1}^{M}\left(\frac{\mathcal{T}}{\tau_0}\right)^{(j-1)}\left|\begin{matrix} 1, 0, \ldots, 0, \ldots, 0; 0, 0, \ldots, 0 \\ \underbrace{0, 0, \ldots, 1}_{m}, \ldots, 0; 0, 0, \ldots, 0 \end{matrix}\right\rangle. \tag{15}$$

Here the index i represents four kinds of wavefunction of the system: (1), both the electron and the hole are in the smaller ring; (2), the hole is in the smaller ring and the electron is in the larger ring; (3), the hole is in the larger ring and the electron is in the smaller ring; (4), both the electron and the hole are in the larger ring. $\mathcal{T}$ is the translation operator defined as

$$\mathcal{T}\left|\begin{matrix} n^{\mathrm{h}}_{11}, n^{\mathrm{h}}_{12}, \ldots, n^{\mathrm{h}}_{1M}; n^{\mathrm{h}}_{21}, n^{\mathrm{h}}_{22}, \ldots, n^{\mathrm{h}}_{2M} \\ n^{\mathrm{e}}_{11}, n^{\mathrm{e}}_{12}, \ldots, n^{\mathrm{e}}_{1M}; n^{\mathrm{e}}_{21}, n^{\mathrm{e}}_{22}, \ldots, n^{\mathrm{e}}_{2M} \end{matrix}\right\rangle = \left|\begin{matrix} n^{\mathrm{h}}_{12}, n^{\mathrm{h}}_{13}, \ldots, n^{\mathrm{h}}_{11}; n^{\mathrm{h}}_{22}, n^{\mathrm{h}}_{23}, \ldots, n^{\mathrm{h}}_{21} \\ n^{\mathrm{e}}_{12}, n^{\mathrm{e}}_{13}, \ldots, n^{\mathrm{e}}_{11}; n^{\mathrm{e}}_{22}, n^{\mathrm{e}}_{23}, \ldots, n^{\mathrm{e}}_{21} \end{matrix}\right\rangle,$$

and $\tau_0 = \mathrm{e}^{\mathrm{i}k}$ is the eigenvalue of $\mathcal{T}$ that corresponds to $|\psi_{2,\tau_0}\rangle$, where k is the propagation number [22]. It is possible to block diagonalize the Hamiltonian where each block has a constant k [16, 22].

Using these base vectors, we can get the Hamiltonian matrix in each k subspace:

$$\mathcal{H}^{(k)}_{2,\tau} = -\begin{pmatrix} H_{11} & H_{12} & H_{13} & H_{14} \\ H^*_{12} & H_{22} & H_{23} & H_{24} \\ H^*_{13} & H^*_{23} & H_{33} & H_{34} \\ H^*_{14} & H^*_{24} & H^*_{34} & H_{44} \end{pmatrix}. \tag{16}$$

Here each $H_{ii'}$ is a $M \times M$ matrix. For the diagonal elements, they have the form

$$\mathcal{H}_{ii} = \begin{pmatrix} p_{1,i} & q_i & 0 & \cdot & 0 & q^*_i \\ q^*_i & p_{2,i} & q_i & 0 & \cdot & 0 \\ 0 & q^*_i & p_{3,i} & q_i & 0 & \cdot \\ \cdot & \cdot & \cdot & \cdot & \cdot & \cdot \\ q_i & 0 & \cdot & 0 & q^*_i & p_{M,i} \end{pmatrix}. \tag{17}$$

Here $p_{j,1}$ is determined by the particle's deflection and the Coulomb potential, $p_{j,2} = 0$, $p_{j,3} = 0$, $p_{1,4} = \gamma$, $p_{j,4} = 0$ (for $j \neq 1$), and

$$q_1 = t^{\parallel}_1(1 + \mu\mathrm{e}^{\mathrm{i}k})\mathrm{e}^{\mathrm{i}2\pi\varphi_1/M}, \tag{18}$$

$$q_2 = t^{\parallel}_2\mathrm{e}^{\mathrm{i}2\pi\varphi_2/M} + t^{\parallel}_1\mu\mathrm{e}^{\mathrm{i}k}\mathrm{e}^{\mathrm{i}2\pi\varphi_1/M}, \tag{19}$$

$$q_3 = t^{\parallel}_2\mu\mathrm{e}^{\mathrm{i}k}\mathrm{e}^{\mathrm{i}2\pi\varphi_2/M} + t^{\parallel}_1\mathrm{e}^{\mathrm{i}2\pi\varphi_1/M}, \tag{20}$$

$$q_4 = t^{\parallel}_2(1 + \mu\mathrm{e}^{\mathrm{i}k})\mathrm{e}^{\mathrm{i}2\pi\varphi_2/M}. \tag{21}$$

All of the off-diagonal elements in equation (16) have the diagonal form, $H_{12} = H_{34} = t^{\perp}_{\mathrm{e}}\mathrm{e}^{\mathrm{i}2\pi\varphi_{\mathrm{e}}}\mathbf{I}$, $H_{13} = H_{24} = t^{\perp}_{\mathrm{h}}\mathrm{e}^{\mathrm{i}2\pi\varphi_{\mathrm{h}}}\mathbf{I}$, $H_{14} = H_{23} = \mathbf{0}$.

The dependence of the eigenvalues on the propagation number, k, has been studied thoroughly in [16, 22, 18], so in this paper, we will not take into account the influence of k on the eigenvalues of the system and choose $k = 0$ in the numerical computation. We can get the energy level distribution and the corresponding state vectors of the system by diagonalizing the Hamiltonian matrix.

3. Numerical results and discussion

For a fixed system, which means the properties of the material that makes up the nanorings, the geometrical parameters of the system and the intensity of the external magnetic field are all known, all the parameters in the Hamiltonian matrix can be calculated. The parameters that can be varied are: the intensity of the external magnetic field, the radii of the two rings, the thickness of the GaAs spacer, the concentration of In in the nanorings and the thickness of the two rings in the z direction, h. The material parameters used in the calculation are summarized in table 1. The number of sites, M, is chosen to be 20. The typical thickness of the rings used is 1 nm [3, 15], the concentration of In $x = 0.60$ and the intensity of the interaction $\gamma_0 = 1.0$ [16].

Table 1. Parameters of $\mathrm{In}_x\mathrm{Ga}_{1-x}\mathrm{As}$ used in the calculation. Unless noted, values are from [23].

Quantity	$\mathrm{In}_x\mathrm{Ga}_{1-x}\mathrm{As}$
E_{g} (eV)	$0.477x^2 - 1.579x + 1.519$
Δ_{SO} (eV)	$0.477x^2 - 0.428x + 0.341$
E_{p} (eV)	$-7.3x + 28.8$
F	$-0.96x - 1.94$
m_0/m^*_{e}	$(1 + 2F) + \frac{E_{\mathrm{p}}(E_{\mathrm{g}} + \frac{2}{3}\Delta_{\mathrm{SO}})}{E_{\mathrm{g}}(E_{\mathrm{g}} + \Delta_{\mathrm{SO}})}$
E_{CBO} (eV)	$0.96x - 0.1x^2$ ([24])
γ_1	$20.0x + 6.98(1 - x)$ ([25])
γ_2	$8.5x + 2.06(1 - x)$ ([25])
γ_3	$9.2x + 2.93(1 - x)$ ([25])
m_0/m^*_{hh}	$\gamma_1 - 2\gamma_2$

3.1. AB oscillations

In figure 2, we plot the flux dependence of the exciton's energy which clearly shows the AB oscillation. From figure 2(a), we find the amplitudes of the oscillation for the ground and first excited states are about 1 and 7 meV. Compared with the AB oscillation of the same system neglecting the Coulomb interaction, figure 2(b), which shows amplitudes about 5 and 15 meV, the amplitudes are significantly suppressed. Moreover this suppression is significantly different for the ground state and the first excited state. For the first excited states, the energy values of the lowest points are unchanged. But for the ground state, the energy level is totally lowered with the emergence of the interaction between the electron and the hole. It is also found that the Coulomb potential leads to the vanishing of the level-crossing between the ground states and the first excited states and the formation of an energy gap between them.

The reason for all these phenomena is the variation of binding states of particles as plotted in figure 3. The origin of the AB oscillation is the finite size of the exciton [9], here, corresponding to the coefficients of basic wavevectors. Because the small ring corresponds to the easy hopping case (larger $t^{\parallel}$), the ground state corresponds to the tight binding state in the small ring, which means the coefficient of ψ^1_1 is much larger than that of the others, figure 3(a). With increasing intensity of Coulomb interaction, on one hand, the absolute value of the interacting part of the total energy becomes larger, which corresponds to the phenomena of the decrease of the system's ground state energy. On the other hand, the kinetic part of the individual particle's energy, corresponding to the AB oscillation, becomes smaller because it becomes more and more difficult for individual particles to escape from the attractive potential, which means a decrease of the amplitude of the AB oscillation. In fact, if γ_0 is chosen to be 2.0, the amplitude of the ground state energy becomes smaller than

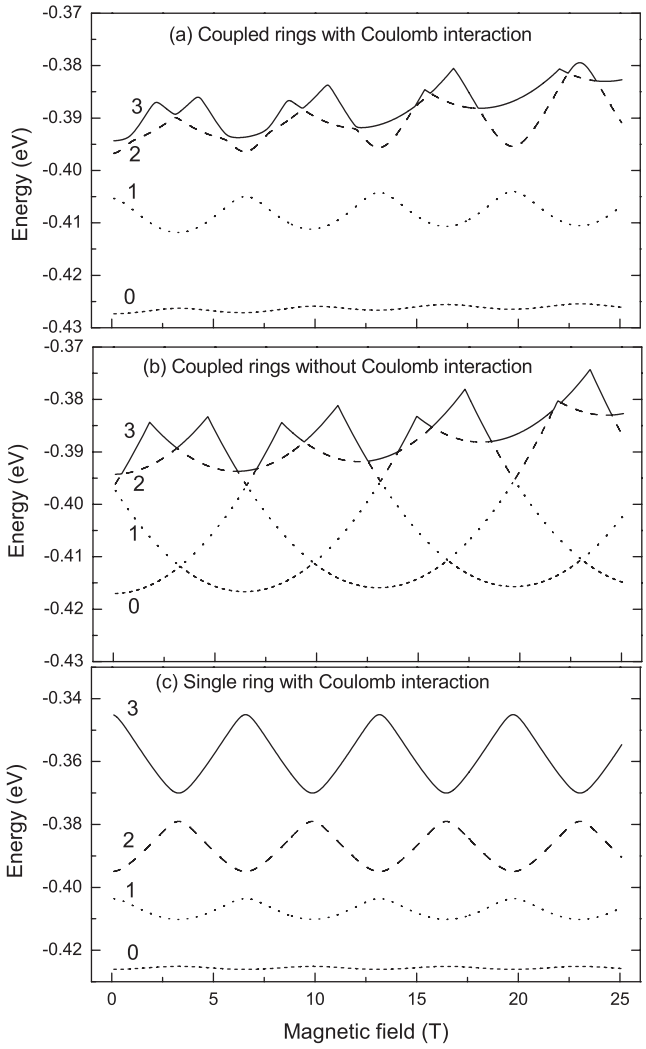

Figure 2. Dependence of the exciton's energy on the flux. The parameters used are $r_1 = 10$ nm, $r_2 = 14$ nm, $d = 3$ nm. In (a), we plot the energy of ground state and three excited states with $\gamma_0 = 1.0$. In (b), the parameter γ_0 is chosen to be zero. In (c), for the convenience of comparison with our model, we plot the ground state energy of a single ring with radius $r_1 = 10$ nm and $\gamma_0 = 1.0$.

0.2 meV, which is comparable to the correction of the ground state energy caused by the coupling of the two rings.

On the contrary, the states for the lowest points of the first excited states correspond to the relatively free kinetic movement of the electron and the hole, which means the coefficient of ψ_1^1, corresponding to the influence of Coulomb interaction, can be approximately taken as zero as in figure 3(c). So the increase of γ_0 will not influence the system's energy at these magnetic field.

In figure 3(b), it is interesting that the largest coefficient is not that of the ψ_1^1, but the ψ_2^1. The reason for this phenomenon is the deflection of particles introduced by the magnetic field. According to our computation, the value of this deflection is just above $\Delta d/2$ at 6.5 T, which means the ψ_2^1 represents the state with Coulomb interaction in our model.

At higher excited states, unlike the discrete energy levels of single rings, figure 2(c), level-crossing emerges when coupling is taken into account, figure 2(a). The reason for this phenomena is the overlapping of two series of energy levels which are determined by the arrangement of the electron and the hole. The level-crossing points represent the changing of different types of system's wavefunction defined above. For example, to the second excited states, before about $B = 6.0$ T the electron is mainly confined in the small ring and the hole is in the large ring, figure 3(e), which represents the third type vector; after the crossing point, both the electron and the hole are confined in the smaller ring, figure 3(f), which is the first type vector.

3.2. Geometrical parameters of the system

The exponential form of $t_{n,i}^{\perp}$ in equation (8) requires the difference of the radii of the two rings and the thickness of the GaAs layer to be small for a significant coupling effect. In figure 4, we plot the dependence of the system's energy on the radius of the large ring. It is clearly shown that when the large ring's radius is smaller than 14 nm, which means the difference of radii is smaller than 4 nm, the system's energy changes significantly with the variation of the radius. Then, if the radius difference of the two rings is larger than 4 nm, continuing to increase the large ring's radius will not change system's energy for the three lowest energy levels. The reason for the fast increase of the system's energy at small radius difference is the sharp decrease of the coupling intensity between two rings, which means a fast increase of the system's energy led by a much stronger confinement condition. For the lowest states, when the difference of radii is above 4 nm, the coupling between two rings is so small that the probability for the particles in the large ring can be taken as zero, so increasing the radius of the large ring will not lead to a variation of the system's energy.

However, for the higher excited level, after the fast increasing region, it experiences a smooth increase then decays to a constant at larger radius, as plotted in figure 4. The reason for this phenomenon is that this state mainly represents the third type of wavefunction as pointed out above, which means the electron and the hole are mainly confined in different rings. The smoothly increasing region represents decoupling of the two rings for the electron. The hole is totally confined in the large ring at small radius difference because of the great influence of its larger effective mass on τ in equation (9). This decoupling process coincides with the description of coupling in [15]. At large radius difference, the coupling can be taken as zero, which means the system can be taken as two independent single rings, each containing one particle. So at large radius difference, the energy of the electron will not be influenced by the change of the large ring's radius. For the hole in the large ring, on one hand, its magnetic flux increases with the enlargement of the ring, which means energy oscillation with an increase of the large ring's radius. On the other hand, the amplitude of the hole's oscillation decreases with an increase of the large ring's radius [16]. Then the system's energy decays to a constant with this increasing as it is the summation of these two parts of energy.

In figure 5, we plot the dependence of the system's ground state energy on the small ring's radius at different values

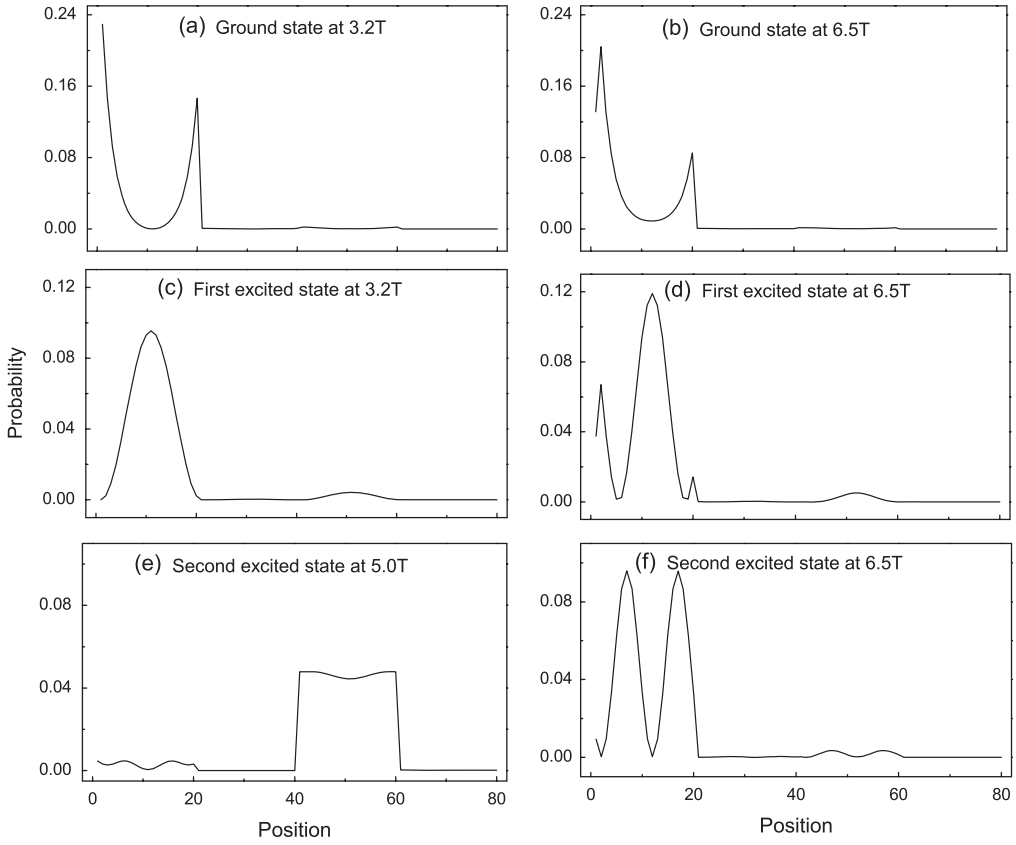

Figure 3. Normalized probability of basic vectors at different magnetic fields. The parameters used are $d = 3$ nm, $r_1 = 10.0$ nm, $r_2 = 14.0$ nm. In (a), we plot the probability of basic vectors of the ground state at 3.2 T, which corresponds to the peak of the ground state's level, and in (b) we plot that at 6.5 T corresponding to the lowest point. In (c) and (d) we plot that of the first excited state corresponding to the lowest point and peak. In (e) and (f) we plot that of the second excited state at 5.0 and 6.5 T, which correspond to two types of state as we defined above.

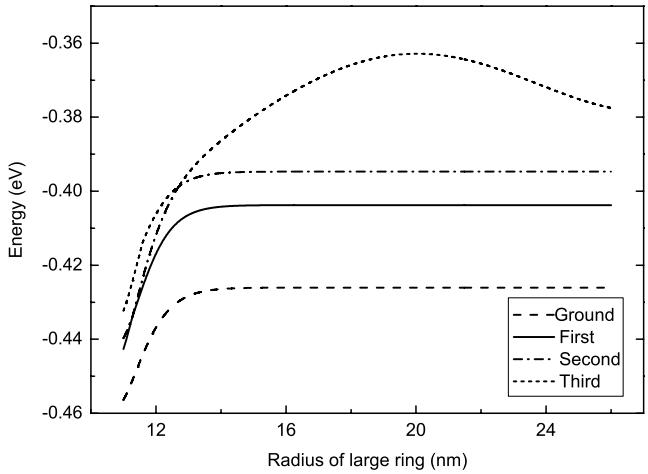

Figure 4. Dependence of the energy on the radius of the larger ring. The parameters are chosen to be $r_1 = 10$ nm, $B = 20.0$ T, $d = 3.0$ nm.

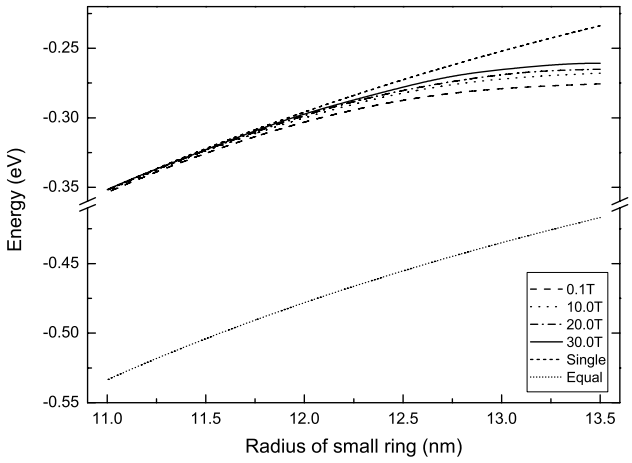

Figure 5. Dependence of the ground state energy on the radius of the small ring. The parameters used are $d = 3.0$ nm, $r_2 = 15$ nm, $B = 0.1$, 10, 20 and 30 T. For the convenience of comparison, we also plot the dependence of the energy on radius for the single ring at $B = 0.1$ T and that for coupling rings with the same radius at $B = 0.1$ T.

of magnetic fields and that for the single ring and coupling concentric rings with same radius. At small r_1, the difference of the system's energy from that of the single ring is negligible because of the weak coupling between rings. However, in the strong coupling region, the difference can reach 45 meV when the radius difference is about 1.5 nm, which is about forty times larger than the amplitude of the AB oscillation.

We also find that this energy difference decreases with increasing magnetic field in figure 5. The reason for this phenomenon is the modulation of the coupling by the magnetic field. At the same radius difference, the cyclotron radius of the electron decreases with the increasing of the magnetic fields, which means the distance of the nearest neighboring sites on different rings is increased, so the coupling is weakened. This phenomenon provides us an opportunity to change the PL spectra by the magnetic field.

Another interesting thing to point out is that the dependence of energy on r_1 does not show an oscillation effect, in figure 5, when the magnetic flux changes with r_1. The reason for this phenomenon is that the amplitude of the AB oscillation for the ground state is too small when being compared with the variation of the energy. For the second and third excited states, which have an amplitude about 10 meV, we can get a modulated oscillation behavior when increasing r_1. But for the higher excited states, because of the level-crossing, it becomes difficult to get a clear oscillation behavior.

The results we get for the energy difference from that of the single ring, which is caused by the coupling effect, coincides with the experimental work in [3]. We find the energy difference is about 45 meV when the difference of the radii is 1.5 nm. In [3], when the GaAs spacer is 3 nm, this difference is about 50 meV. Just as Granados *et al* [3] pointed out, the decrease of the energy is caused by the coupling between rings. Moreover, we find the coupling between rings with different radii is the dominant part of the coupling effect because the coupling between rings with same radius can only lead to a constant difference of about 0.18 eV and this deflection is almost unchanging with variation of the radius and much larger than the data in [3].

In figure 6, we plot the influence of the GaAs spacer on the system's energy at different magnetic fields. Because of the exponential form of τ in equation (9), the spacer's thickness can greatly influence the cyclotron radii of the electron and the hole, which will lead to a variation of the system's energy.

From figure 6, we find the energy levels can be divided into three regions for each magnetic field: two fast increasing regions and the constant region. The reason for both of these increases of the system's energy is the decoupling between rings. Because of the great difference on τ led by β in equation (9), the spacer's thickness at which the hole's cyclotron radius becomes smaller than the radius difference is much smaller than that for the electron. So the hole is totally confined in the small ring at a relatively small thickness of the GaAs spacer, which corresponds to the 'A' points in figure 6. On the other hand, with an increase of the spacer's thickness, the electron is also more and more confined in the small ring. At the 'B' points, the electron is also totally confined in the small ring, which represents the decoupled points of the rings. After these points, an increase of the spacer's thickness will not influence the system's energy, which corresponds to the constant region where we can take this system as two independent rings. It is interesting that the thickness of the GaAs spacer at which the electron (hole) shows totally decoupled phenomena coincides with the data in [15].

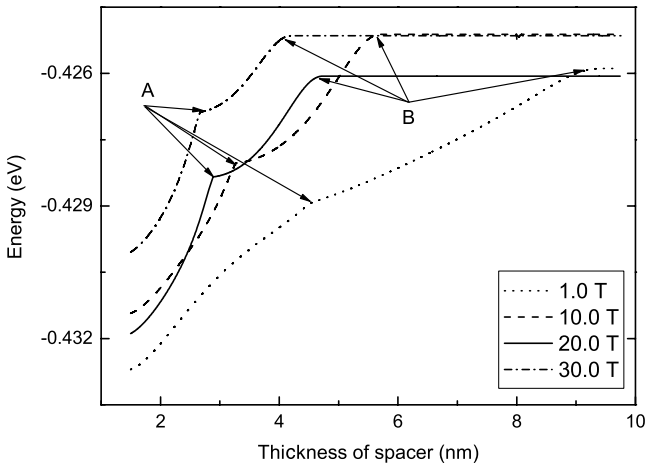

Figure 6. Dependence of the ground state energy on the thickness of the spacer. The parameters used are $r_1 = 10$ nm, $r_2 = 13$ nm, $B = 1.0$, 10.0, 20.0 and 30.0 T.

From figure 6, we find the energy region of the AB oscillation can be changed by modulating the spacer's thickness. For every value of the spacer's thickness, the energy at a certain magnetic field corresponds to one point on the AB oscillation. So the largest distance between these values provides us the energy region we can get by changing the magnetic field. From figure 6, this region can be several times larger than the amplitude of the AB oscillation, which is the result of the modulation of coupling by the magnetic field, as pointed out above. On the other hand, by changing the thickness of the spacer, we can get the energy region of the AB oscillation we want.

4. Conclusions

In conclusion, we have studied the influence of geometric parameters and that of the coupling on the AB oscillation in concentric double nanorings by the attractive Fermionic Hubbard model. According to our results, the amplitude of the AB oscillation is strongly influenced by the intensity of the Coulomb potential and the energy levels decrease with the emergence of the coupling between rings. This coupling also leads to the level-crossing of the high excited states.

By modulating the radii of the two rings, we can change the values of the energy levels. In the strong coupling region, the energy levels increase sharply with an increase of the larger ring's radius. In the weak coupling region, the lowest energy levels remain unchanged and the high excited level exhibits a decaying behavior. With the variation of the small ring's radius, in the strong coupling region, the energy difference from the energy of the single ring decreases with an increase of the magnetic field; in the weak coupling region, the system's energy is almost the same as that of the single ring.

By changing the thickness of the GaAs spacer, we can modulate the coupling of the two rings, which has a great influence on the system's energy. At the different magnetic fields, there are two fast increasing regions, corresponding to the decoupling for the hole and the electron, and a constant

region, corresponding to uncoupled region. We also predict that by changing the thickness of the GaAs spacer, the energy region of the AB oscillation can be modulated.

Acknowledgments

This work was supported by the National Natural Science Foundation of China (Grant Nos 10674058, 60371013) and the State Key Program for Basic Research of China (Grant No. 2006CB921803).

References

[1] Warburton R J, Schäflein C, Haft D, Bickel F, Lorke A, Karrai K, García J M, Schoenfeld W and Petroff P M 2000 *Nature* **405** 926
[2] Granados D and García J M 2003 *Appl. Phys. Lett.* **82** 2401
[3] Granados D, García J M, Ben T and Molina S I 2005 *Appl. Phys. Lett.* **86** 071918
[4] Mano T, Kuroda T, Sanguinetti S, Ochiai T, Tateno T, Kim J, Noda T, Kawabe M, Sakoda K, Kido G and Koguchi N 2005 *Nano Lett.* **5** 425
[5] Lorke A, Luyken R J, Govorov A O, Kotthaus J P, García J M and Petroff P M 2000 *Phys. Rev. Lett.* **84** 2223
[6] Bayer M, Korkusinski M, Hawrylak P, Gutbrod T, Michel M and Forchel A 2003 *Phys. Rev. Lett.* **90** 186801
[7] Barticevic Z, Fuster G and Pacheco M 2002 *Phys. Rev.* B **65** 193307
[8] Voskoboynikov O, Li Y, Lu H-M, Shih C-F and Lee C P 2002 *Phys. Rev.* B **66** 155306
[9] Römer R A and Raikh M E 2000 *Phys. Rev.* B **62** 7045
[10] Hu H, Zhu J L, Li D J and Xiong J J 2001 *Phys. Rev.* B **63** 195307
[11] Maschke K, Meier T, Thomas P and Koch S W 2001 *Eur. Phys. J.* B **22** 249
[12] Govorov A O, Ulloa S E, Karrai K and Warburton R J 2002 *Phys. Rev.* B **66** 081309(R)
[13] Maslov A V and Citrin D S 2003 *Phys. Rev.* B **67** 121304(R)
[14] Zhang T Y and Cao J C 2005 *J. Appl. Phys.* **97** 024307
[15] Ouerghui W, Martinez-Pastor J, Gomis J, Maaref M A, Granados D and García J M 2006 *Eur. Phys. J.* B **54** 217
[16] Palmero F, Dorignac J, Eilbeck J C and Römer R A 2005 *Phys. Rev.* B **72** 075343
[17] Grochol M, Grosse F and Zimmermann R 2006 *Phys. Rev.* B **74** 115416
[18] Dorignac J, Eilbeck J C, Salerno M and Scott A C 2004 *Phys. Rev. Lett.* **93** 025504
[19] Stafford C A, Kotlyar R and Das Sarma S 1998 *Phys. Rev.* B **58** 7091
[20] Anwar A F M, Khondker A N and Khan M R 1989 *J. Appl. Phys.* **65** 2761
[21] Thanikasalam P and Venkatasubramanian R 1993 *IEEE J. Quantum Electron.* **29** 2451
[22] Scott A 2000 *Quantum Lattice Solitons* (Berlin: Springer)
[23] Vurgaftmana I, Meyer J R and Ram-Mohan L R 2001 *J. Appl. Phys.* **89** 5815
[24] Zubkov V I, Melnik M A, Solomonov A V and Tsvelev E O 2004 *Phys. Rev.* B **70** 075312
[25] Nakaoka T, Saito T, Tatebayashi J and Arakawa Y 2004 *Phys. Rev.* B **70** 235337